Journal of ELECTRONIC MATERIALS, Vol. 40, No. 8, 2011
DOI: 10.1007/s11664-011-1690-1

Effects of Varying MBE Growth Conditions on Layered Zn-Se-Te Structures

BIDISHA ROY,[1,4,5] AIDONG SHEN,[2] MARIA C. TAMARGO,[3,4] and IGOR L. KUSKOVSKY[1,4]

1.—Department of Physics, Queens College of CUNY, 65-30 Kissena Blvd, Flushing, NY 11367, USA. 2.—Department of Electrical Engineering, The City College of CUNY, 160 Convent Avenue, New York, NY 10031, USA. 3.—Department of Chemistry, The City College of CUNY, Convent Avenue at 138th Street, New York, NY 10031, USA. 4.—The Graduate Center, CUNY, 365 5th Avenue, New York, NY 10016, USA. 5.—e-mail: bidisha@physics.qc.cuny.edu

We report the effects of varying growth parameters on the photoluminescence (PL) and time-resolved photoluminescence (TRPL) emission from layered Zn-Se:Te structures with submonolayer quantities of ZnTe grown by a combination of migration-enhanced epitaxy (MEE) and molecular beam epitaxy (MBE). Dependences on Te effusion cell temperature ($T_{\text{Te source}}$) and "wait time" (duration for which all shutters are closed, $t_{\text{all-off}}$) are investigated to show that these parameters contribute towards changing the size and/or composition of the quantum dots (QDs). Optical studies showed that increasing $T_{\text{Te source}}$ resulted in the formation of larger QDs. Increasing $t_{\text{all-off}}$ from 0 s to 3 s contributed towards the formation of larger QDs, while further increasing $t_{\text{all-off}}$ to 9 s led to desorption of Te adatoms which resulted in smaller QDs. These parameters are easy to control, and thus understanding their effects should help us to gain better control towards obtaining high-quality QDs.

Key words: Type II QDs, Zn-Se-Te, submonolayer, MBE, effusion cell, II–VI compounds, photoluminescence

INTRODUCTION

In type II semiconductor heterostructures, due to staggered band alignment, the material with the lower potential energy for electrons has the higher potential energy for holes and vice versa, leading to spatial separation of photogenerated electrons and holes. This results in long carrier recombination lifetimes and causes dependence of photoluminescence (PL) and photocurrents on the intensity of excitation as well as on the external electric and magnetic field.[1–3] These properties can be used for new and enhanced material characteristics and devices.

Among semiconductor heterogeneous systems with type II band alignment, Zn-Se-Te has been studied for its interesting optical properties (see Refs. [3–5] and references therein). There is also a possibility of using doped ZnTe/ZnSe (or similar alloys) quantum dots (QDs) for development of more efficient quantum dot infrared photodetectors (QDIP), as the carrier confinement in type II systems is independent of the band gaps of the underlying materials, but rather depends on the band offsets, and can be engineered to fit a required wavelength region. In addition to being type II, the QD system discussed herein (Zn-Se-Te) is grown without a wetting layer (WL), which is one of the culprits of poor performance of many QDIPs.[6] Such advantages can be useful for industries related to defense applications and telecommunication.

By tuning the dot size, chemical composition, and doping levels, one should be able to adjust the optical transitions to desired wavelengths. Obtaining high-quality, controlled growth of QDs with

(Received November 14, 2010; accepted May 25, 2011; published online June 22, 2011)

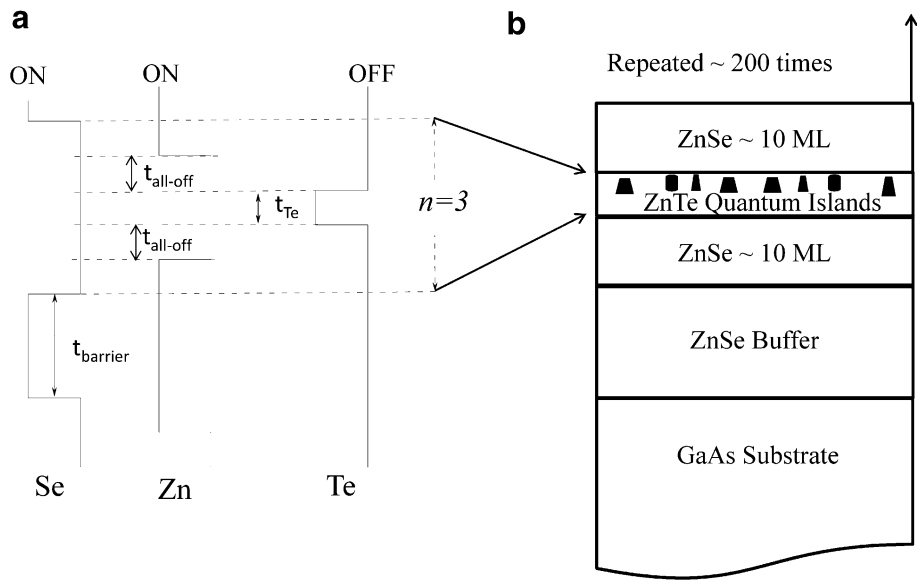

Fig. 1. Schematics of (a) shutter sequence for sample growth, and (b) sample structure.

uniform size distribution still remains a challenge, being one of the prime requirements that may provide adequate spectral response with lesser inhomogeneous broadening and improved performance of QD-based devices. However, to attain better control and ensure progress, it is important to understand the fundamental properties and also the growth mechanisms of these materials. Herein, we report results of our efforts to study the effects of changing MBE growth conditions with the goal of controlling the size and chemical composition of the QDs in layered Zn-Se-Te structures.

EXPERIMENTAL PROCEDURES

Multilayered Zn-Se-Te structures with submonolayer quantities of ZnTe were grown by a combination of migration-enhanced epitaxy (MEE)* and MBE in a Riber 2300 system. Samples were grown on (001) GaAs substrates. Prior to the growth of the II–VI epilayers, Zn irradiation of the GaAs surface was performed for ~20 s at 200°C. Then, an undoped ZnSe buffer layer was grown at 300°C under Se-rich conditions. After the buffer layer growth, the multilayers were grown. A 10-monolayer-thick ZnSe spacer (barrier) was grown by opening the Zn and Se shutters together, after which the Se shutter was closed to produce a Zn-terminated surface. Then, all shutters were closed to desorb excess Zn from the surface. The Te shutter was opened for 5 s to deposit Te onto the Zn-terminated surface. This was followed by closing of all shutters for $t_{\text{all-off}}$ seconds, followed by opening of the Zn shutter to produce another Zn-terminated surface. This wait time ($t_{\text{all-off}}$) was chosen as one of the varied parameters. Four values (0 s, 3 s, 6 s, and 9 s) were tried, forming sample series II (see below) for this work. We note that Te (Zn) was deposited without Zn (Te), which enhances surface diffusion. Since a very small Te flux is used during the deposition, only a fraction of a Te monolayer (submonolayer) is formed, which leads to the formation of type II QDs. [The lack of full ZnTe monolayers is also supported by monitoring the reflection high-energy electron diffraction (RHEED) oscillations during the growth.] This procedure was repeated three times, before the Se shutter was again opened to start the next growth sequence. The whole cycle was repeated for ~100 to 200 periods. More details on the growth procedure are described elsewhere (see, e.g., Ref. 5). Figure 1a and b illustrate the shutter sequence during the growth procedure and a schematic sample structure, respectively. Two different series of samples were grown, as briefly discussed above and summarized in Table I. For series I (samples A, B, and C) the Te effusion cell temperature ($T_{\text{Te source}}$) was varied during the growth, whereas, for series II (D, F, E, and G), samples were grown by varying the wait time ($t_{\text{all-off}}$ after the Te shutter was opened) while following the shutter sequence.

For PL measurements, the 351 nm emission line from an Ar^+ laser was used for excitation. The PL emission was detected by a TriVista SP2 500i triple monochromator coupled to a thermoelectrically cooled photomultiplier tube (PMT) and a photon counting system. Time-resolved PL (TRPL) studies were performed using the 337 nm line of a N_2 pulsed laser with 4 ns pulse width. The signal was recorded using a 500 MHz Tektronix TDS 654C oscilloscope. The excitation intensity was varied

*Migration-enhanced epitaxy is a variant of conventional MBE, occurring when the growing surface is alternately exposed to group II and group VI elements or to group III and group V elements. For a review, see, e.g., Ref. 7.

Table I. Sample information with varied growth parameters

Series I			Series II		
Sample	**$T_{Te\ source}$**	**PL Peak Energy (at 10 K)**	**Sample**	**$t_{all\text{-}off}$**	**PL Peak Energy (at 10 K)**
A	215°C	2.680 eV	D	0 s	2.430 eV
B	225°C	2.474 eV	E	3 s	2.411 eV
C	245°C	2.285 eV	F	6 s	2.414 eV
			G	9 s	2.460 eV

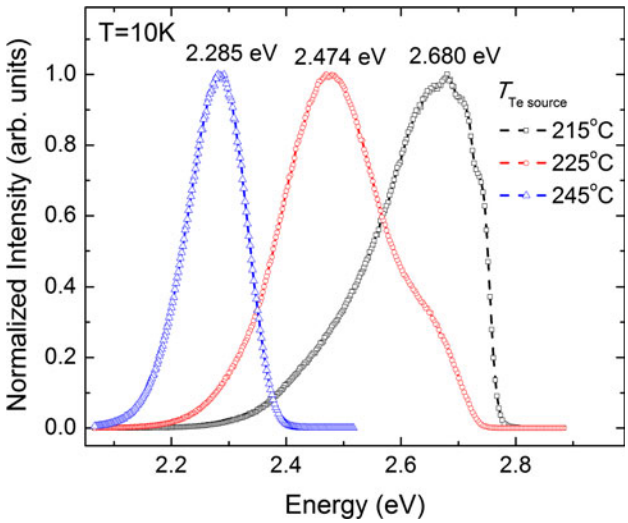

Fig. 2. Low-temperature PL of ZnTe/ZnSe QDs as a function of $T_{Te\ source}$.

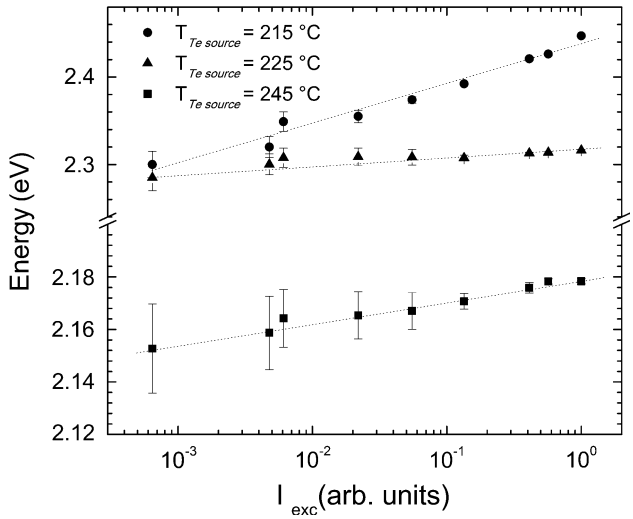

Fig. 3. Excitation intensity (I_{exc}) dependence of emission energy at 20% height of the peak on the low-energy side for sample series I with varied $T_{Te\ source}$. Dotted lines are guides to the eye.

over three orders of magnitude using neutral-density filters. A temperature-variable ARS closed-cycle refrigerating system with He compressor was used for low-temperature and temperature-dependent measurements from 7 K to 250 K for both continuous-wave (cw) and time-resolved PL measurements.

RESULTS AND DISCUSSION

The PL spectra at 10 K for samples A, B, and C with increasing Te effusion cell temperature ($T_{Te\ source}$) are shown in Fig. 2. The corresponding peaks are observed at ~2.680 eV, 2.474 eV, and 2.285 eV. We propose that the red-shift of the peak position from sample A to C correlates with the higher $T_{Te\ source}$, i.e., higher Te beam intensity,[8] which leads to the formation of larger nanoislands.** This is supported by the fact that samples A and B show the presence of two broad PL peaks (and some other characteristic sharp features) when studied carefully; these latter features (~2.70 eV and 2.73 eV) present at the higher-energy side are characteristic of relatively low Te fraction in the sample.[4,5,11] A high energy band ("blue") between 2.60 eV and 2.75 eV, and a lower energy band ("green") at ~2.50 eV are clearly present. The blue band is generally accepted to be due to the emission from excitons bound to isoelectronic Te_2 complexes. The green band is attributed to emission from excitons both bound to isoelectronic $Te_{n\geq 2}$ clusters and confined to type II QDs.[4,11] Contribution from a peak near the tail of the green band, between ~2.2 eV and 2.3 eV, is also present in the PL spectra of samples B and C, which is a result of larger, Te-rich, ZnTe QDs.[11,12] The PL peak of sample C at ~2.28 eV shows the absence of the higher-energy peaks and is narrower. This peak is thus mainly due to larger QDs with a more uniform size distribution than in samples A and B.

The excitation intensity dependence of the emission energy at 20% height of the peak on the low-energy side of samples A, B, and C is shown in Fig. 3. The blue-shift of the emission energy with increasing excitation intensity has been previously reported for various type II quantum structures.[13–15] For our material system of ZnTe/ZnSe QDs, due to a large valence-band offset (0.8 eV to

**We propose that the larger Te beam intensity contributed primarily towards increasing the size of the QDs. The concentration of Te in these samples is estimated to be between 50% and 70%, see Refs. 9,10. The red-shift in peak position strengthens our proposition regarding the composition estimation, as in case of increase in Te concentration over 60%, the peak position is expected to show a blue-shift.

1.0 eV), the hole is strongly confined within the ZnTe-rich QD whereas the electron is located within the ZnSe-rich barriers. The Coulomb interaction creates an electric field across the interface which results in band bending. On increasing the excitation intensity, more electron and hole pairs are excited and the band-bending effect is increased. The emission spectra thus shift to higher energies with increasing excitation intensity, and this effect is at least partially attributed to type II quantum structures. We also note that the magnitude of the shift in emission energy on changing the excitation intensity over three orders of magnitude is largest for sample A (~147 meV) followed by samples B (~31 meV) and C (~26 meV). We attribute this observation to be an indication of the size of the QDs. Larger QDs have closely spaced energy levels, and on changing the excitation intensity, the relative change in energy levels for the carriers is smaller for larger QDs, and thus the smaller QDs show a larger shift as compared with that shown by larger QDs for the same amount of change in excitation intensity. This supports our conclusion that the size of the QDs increased from sample A to B and further in sample C due to increasing $T_{\text{Te source}}$.

Figure 4a and b show the low-temperature TRPL for samples A and B taken at the same energy of 2.38 eV and for samples B and C at 2.33 eV, respectively. Sample A shows faster decay than sample B, which is indicative of smaller QDs in sample A. This is explained by lifetime being dependent on the overlap of the carrier wavefunctions, which is larger for smaller QDs. This also supports our observation of a red-shift of PL peak position of sample B with respect to sample A. At the same time, Fig. 3b indicates that sample C exhibits faster recombination lifetime in comparison with sample B. Although this is counterintuitive and not well understood, we point out that such a behavior of PL lifetime at low energy (<2.35 eV) in Zn-Se-Te systems has been previously reported and is tentatively attributed to impurities or defect states formed on the QD surface, the origin of which may be related to strain relaxation of larger QDs due to strain interaction of the coupled QD layers.[11] This is reported to increase dislocation and defect formation significantly in InAs QDs.[16] Such dislocations will significantly decrease the PL lifetime of the QDs due to an increased contribution from nonradiative processes. Previously, this low-energy emission was mixed with other processes in one sample, rather than being dominant as seen here, and we thus plan further studies of this matter.

The 10-K PL results for sample series II with different wait-time durations, i.e., time for which all the shutters are off ($t_{\text{all-off}}$), are shown in Fig. 5. The PL peaks for samples D, E, F, and G are observed at 2.430 eV, 2.411 eV, 2.414 eV, and 2.460 eV, respectively. We discuss such an observation in terms of $t_{\text{all-off}}$ affecting the competition between surface diffusion of Te adatoms (which is responsible for the

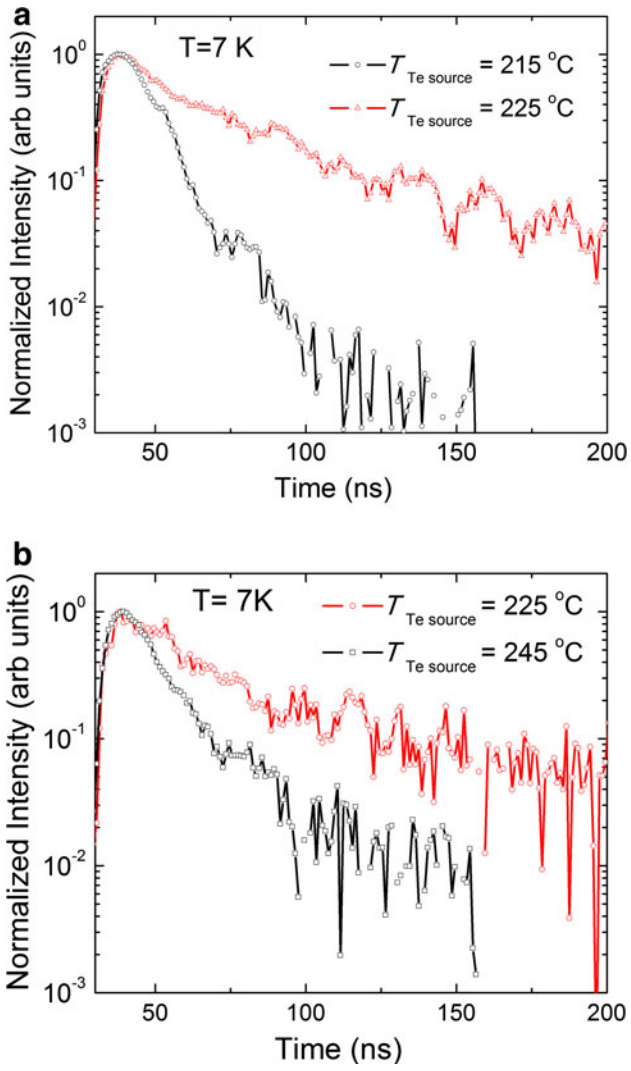

Fig. 4. (a) TRPL of ZnTe/ZnSe QDs grown with $T_{\text{Te source}}$ = 215°C and 225°C. (b) TRPL of ZnTe/ZnSe QDs for $T_{\text{Te source}}$ = 225°C and 245°C.

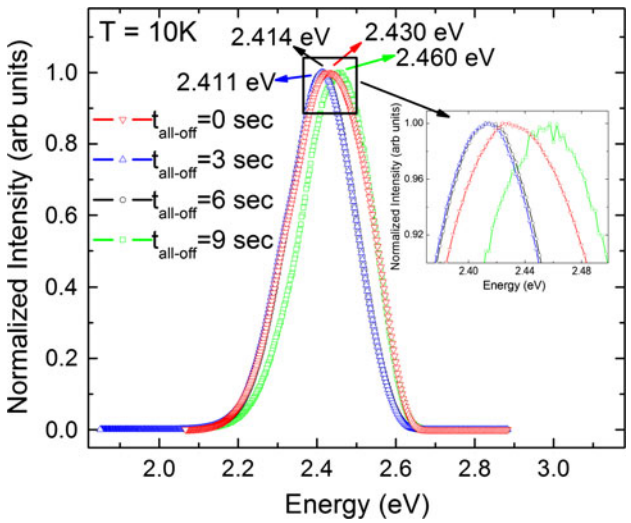

Fig. 5. Low-temperature PL of ZnTe/ZnSe QDs grown with different $t_{\text{all-off}}$.

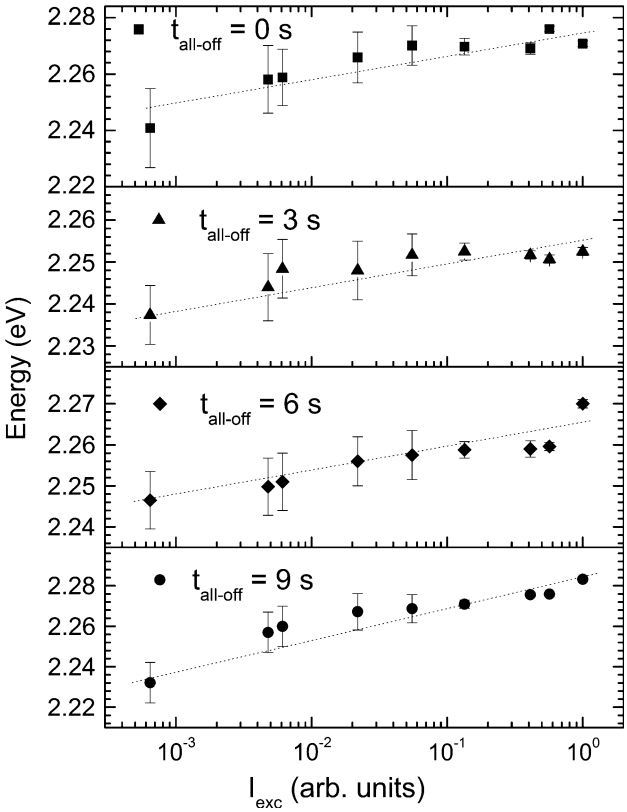

Fig. 6. Excitation intensity (I_{exc}) dependence of the emission energy at 20% height of the peak on the low-energy side for samples in series II for different $t_{all\text{-}off}$. Dotted lines are guides to the eye.

formation of the QDs) and their desorption.[17] We estimate that, for $t_{all\text{-}off}$ between 0 s and 3 s, diffusion of Te adatoms leads to their aggregation into nanoislands, thus allowing formation of larger QDs (shown by the red-shift in the peak position of samples D and E of ~19 meV). Increasing $t_{all\text{-}off}$ from 3 s to 6 s results in the PL blue-shift (~3 meV for samples E and F), indicating onset of desorption of Te adatoms. Further increasing $t_{all\text{-}off}$ to 9 s showed a significant blue-shift (~46 meV) of the PL for samples F and G, which we explain as being due to increased desorption of Te adatoms and thus a decrease in size or loss of QDs.

This sample series also exhibits the blue-shift of emission energy taken at 20% height of the peak on the low-energy side with increasing excitation intensity over three orders of magnitude (Fig. 6). As explained above, this is due to the presence of type II QDs where the band bending and the generation of excited carriers are dependent on the excitation intensity. The higher the excitation intensity, the larger the band bending and the higher the PL peak position, observed as the blue-shift. As explained above, the magnitude of the emission energy shift may be seen as an indication of the size of the QDs. The shift is largest in sample G (~53 meV) followed by that in sample D (~29 meV). Samples E (~15 meV) and F (~23 meV)

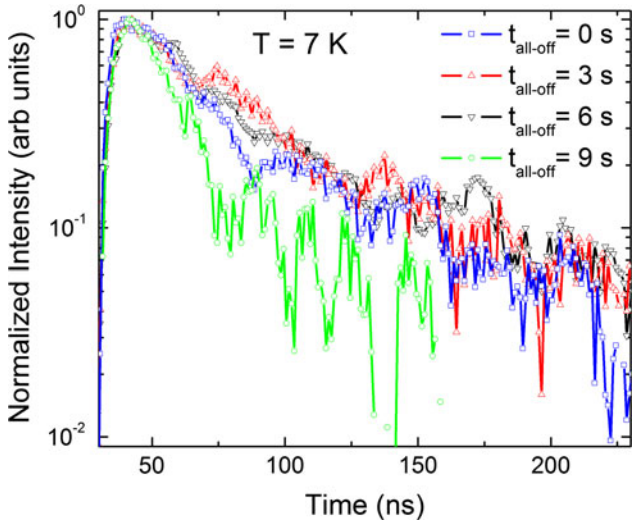

Fig. 7. TRPL of ZnTe/ZnSe QDs to compare lifetimes for samples from series II.

show a smaller shift in the emission energy. This strengthens our proposition that smaller to larger QDs are present in samples G, D, F, and E, respectively. The excitation intensity dependence of the PL emission can also be accounted for in terms of relative change in carrier concentration with varying excitation intensity, taking into account that the volume density of carriers is higher for smaller QDs at higher excitation intensity as compared with that of the larger QDs.

The low-temperature TRPL lifetimes for sample series II are shown in Fig. 7. Sample G exhibits faster decay, with samples D, E, and F showing subsequently slower decays. This confirms the presence of smaller QDs in sample G due to the loss of Te adatoms through the process of desorption, while samples E exhibit relatively longer lifetime as expected, due to formation of larger QDs as a result of diffusion and aggregation of Te adatoms.

CONCLUSIONS

We propose that higher $T_{Te\ source}$ facilitated higher Te flux which led to clustering of Te adatoms. We observed a signature of larger QDs formed with $T_{Te\ source}$ = 245°C as compared with $T_{Te\ source}$ = 215°C and 225°C. Also it is shown that, while increasing $t_{all\text{-}off}$ from 0 s to 3 s led to diffusion of Te adatoms and formation of larger dots, further increasing $t_{all\text{-}off}$ up to 9 s resulted in desorption of Te adatoms, leading to smaller QDs. The competition between these two processes determines the size and chemical composition of the QDs. Low-temperature PL and excitation intensity-dependent PL along with TRPL studies support our conclusions.

In the future, we plan to perform high-resolution X-ray diffraction (HRXRD) analysis to compare the structural properties of these samples. Also, to

further study the QDs, we intend to perform electro- and magneto-PL measurements.

ACKNOWLEDGEMENTS

The authors acknowledge the support of the Department of Energy under Grant No. DE-FG02-10ER46678 and PSC CUNY under Grant No. 62548-00 40.

REFERENCES

1. J.R. Madureira, M.P.F. de Godoy, M.J.S.P. Brasil, and F. Iikawa, *Appl. Phys. Lett.* 90, 212105 (2007).
2. C.Y. Jin, H.Y. Liu, S.Y. Zhang, Q. Jiang, S.L. Liew, M. Hopkinson, T.J. Badcock, E. Nabavi, and D.J. Mowbray, *Appl. Phys. Lett.* 91, 021102 (2007).
3. I.L. Kuskovsky, W. MacDonald, A.O. Govorov, L. Muroukh, X. Wei, M.C. Tamargo, M. Tadic, and F.M. Peeters, *Phys. Rev. B* 76, 035342 (2007).
4. Y. Gu, I.L. Kuskovsky, M. van der Voort, G.F. Neumark, X. Zhou, and M.C. Tamargo, *Phys. Rev. B* 71, 045340 (2005).
5. I.L. Kuskovsky, C. Tian, G.F. Neumark, J.E. Spanier, I.P. Herman, W.C. Lin, S.P. Guo, and M.C. Tamargo, *Phys. Rev. B* 63, 155205 (2001).
6. J. Phillips, *J. Appl. Phys.* 91, 4590 (2002).
7. Y. Horikoshi, *Semicond. Sci. Technol.* 8, 1032 (1993).
8. T. Yao, Y. Miyoshi, Y. Makita, and S. Maekawa, *Jpn. J. Appl. Phys.* 16, 369 (1977).
9. Y. Gong, H.F. Yan, I.L. Kuskovsky, Y. Gu, I.C. Noyan, G.F. Neumark, and M.C. Tamargo, *J. Appl. Phys.* 99, 064913 (2006).
10. Y. Gong, W. MacDonald, G.F. Neumark, M.C. Tamargo, and I.L. Kuskovsky, *Phys. Rev. B* 77, 155314 (2006).
11. M.C.K. Cheung, A.N. Cartwright, I.R. Sellers, B.D. McCombe, and I.L. Kuskovsky, *Appl. Phys. Lett.* 92, 032106 (2008).
12. I.R. Sellers, V.R. Whitesides, I.L. Kuskovsky, A.O. Govorov, and B.D. McCombe, *Physica E* 40, 1819 (2008).
13. Y.S. Chiu, M.H. Ya, W.S. Su, and Y.F. Chen, *J. Appl. Phys.* 92, 5810 (2002).
14. E.R. Glaser, B.R. Bennett, B.V. Shanabrook, and R. Magno, *Appl. Phys. Lett.* 68, 3614 (1996).
15. F. Hatami, M. Grundmann, N.N. Ledentsov, F. Heinrichsdorff, R. Heitzouml, J. hrer, D. Bimberg, S.S. Ruvimov, P. Werner, V.M. Ustinov, P.S. Kop'ev, and Zh I. Alferov, *Phys. Rev. B* 57, 4635 (1998).
16. H.Y. Liu, I.R. Sellers, T.J. Badcock, D.J. Mowbray, M.S. Skolnick, K.M. Groom, M. Gutierrez, M. Hopkinson, J.S. Ng, J.P.R. David, and R. Beanland, *Appl. Phys. Lett.* 85, 704 (2004).
17. S. Tatarenko, B. Daudin, and D. Brun-Le Cunff, *Appl. Phys. Lett.* 66, 1773 (1995).